ResearchGate

See discussions, stats, and author profiles for this publication at: https://www.researchgate.net/publication/231629466

Characterization of Protonated Formamide-Containing Clusters by Infrared Spectroscopy and ab Initio Calculations. II. Hydration of Formamide in the Gas Phase

ARTICLE *in* THE JOURNAL OF PHYSICAL CHEMISTRY A · SEPTEMBER 2001

Impact Factor: 2.69 · DOI: 10.1021/jp004103f

CITATIONS
24

READS
16

5 AUTHORS, INCLUDING:

Jyh-Chiang Jiang
National Taiwan University of Science and Te…
174 PUBLICATIONS **2,612** CITATIONS
SEE PROFILE

Chih-Che Wu
National Chi Nan University
28 PUBLICATIONS **667** CITATIONS
SEE PROFILE

Available from: Jyh-Chiang Jiang
Retrieved on: 26 January 2016

Characterization of Protonated Formamide-Containing Clusters by Infrared Spectroscopy and ab Initio Calculations. II. Hydration of Formamide in the Gas Phase

C. Chaudhuri,[†] J. C. Jiang,[†] C.-C. Wu,[‡] X. Wang,[§] and H.-C. Chang*,[†]

Institute of Atomic and Molecular Sciences, Academia Sinica, P.O. Box 23-166, Taipei, Taiwan 106, Department of Chemistry, National Taiwan University, Taipei, Taiwan 106, and State Key Laboratory of Molecular Reaction Dynamics, Dalian Institute of Chemical Physics, Chinese Academy of Sciences, Dalian 116023

Received: November 7, 2000; In Final Form: June 25, 2001

Structures of the solvation shells of O-protonated formamide (H^+FA) have been characterized by infrared spectroscopy and ab initio calculations at varying stages of hydration. A few isomeric structures, including both H^+FA- and H_3O^+-centered forms, were identified from a close examination of the hydrogen-bonded and non-hydrogen-bonded NH and OH stretching spectra of $H^+FA(H_2O)_n$ ($n = 3$ and 4) produced by a supersonic expansion. Theoretical investigations of $H^+FA(H_2O)_{1-3}$ indicate that filling of the first hydration shell of the protonated formamide cation with three water molecules is not an energetically favorable process. The process is hampered by the hydrogen bond anticooperative effect, which prohibits both NH bonds to be involved in hydrogen bonding. Further increasing the cluster size to $n = 4$ results in grouping of the water molecules on one side of the formamide, rather than forming a filled first solvation shell of H^+FA. The grouping, in effect, enhances the proton affinity of the water molecule in direct contact with the excess proton and progressively moves the proton away from H^+FA, producing an H_3O^+ ion core. Detailed analysis of the results, both qualitatively and quantitatively, reveals the existence of a low-barrier proton transfer process, which is expected to occur similarly in aqueous solutions during acid-catalyzed amide hydrolysis. In this work, we also successfully identified a shell-filled isomer for $H^+(FA)_3H_2O$ for the first time. It is demonstrated that a combined investigation of cluster ions by infrared spectroscopy and ab initio calculations allows for an unambiguous determination of both the protonation sites and hydration structures of biomolecules in the gas phase.

Introduction

In studying the physical chemistry of biological molecules in water, formamide (FA) often serves as a model system.[1] This is conceivably because formamide is not only the simplest molecule that contains a peptide bond, but also is the simplest molecule that consists of two functional groups (−CO and $-NH_2$) responsible for nucleic base pairing in DNA. How water interacts with formamide has been a subject of scrutiny by both experimentalists and theorists. Recent calculations,[2−4] in particular, predict that water plays a catalytic role in intramolecular proton transfer between the CO and NH_2 moieties of formamide. Water assists this keto−enol tautomerization, leading from formamide [$HC(O)NH_2$] to formamidinic acid [HC(OH)═NH], by exchanging its own protons with that of formamide. A bridge of the two functional groups by a single water molecule markedly reduces the height of the tautomerization barrier by more than 20 kcal/mol.[3] Similar catalytic effects are also found for the protonated forms of formamide and are expected to play an important role in the fragmentation of electrosprayed protonated peptides in the gas phase.[5]

Apart from the water-assisted keto−enol tautomerization, one important aspect in the studies of formamide-water interactions is amide hydrolysis. Hydrolysis of formamide in neutral water is a slow process, but is greatly accelerated in acidic or basic solutions.[6] Studying the acid- or base-catalyzed processes is considered the first step toward a detailed understanding of enzymatic peptide hydrolysis. For formamide, extensive calculations have been performed to understand its protonation,[7−14] acid-,[7,9] and base-catalyzed hydrolysis.[15] There are two sites available for the protonation to occur on this bidentate base: either oxygen or nitrogen. Both computational[7−14] and spectroscopic studies[16] accordingly indicate that gas-phase formamide prefers O-protonation due to its zwitterionic character.[17] This gas-phase property is expected to be held in solution phases,[18] because the N-protonated intermediate is about 10 kcal/mol higher in free energy than the O-protonated intermediate, as predicted by ab initio calculations and Monte Carlo simulations.[13] The prediction is in line with isotope exchange measurements,[19] which suggest an O-protonation pathway of acid-catalyzed amide hydrolysis.

A prerequisite for thorough understanding of acid-catalyzed peptide hydrolysis in living systems is to obtain information of how a protonated formamide cation is surrounded by water molecules. Such information, concerning the hydration structure and solvation effects, can be deduced from vibrational spectroscopic studies of molecular cluster ions at a microscopic level. For the O-protonated formamide, one reasonable expectation would be that filling the first hydration shell of H^+FA requires three water molecules forming three separate hydrogen bonds with the $-OH$ and $-NH_2$ moieties, while multiple hydrogen bonds could form between them as in the neutral $HC(O)NH_2-H_2O$ binary complex.[20] Using mass spectrometry, Meot-

*Corresponding author. E-mail: hcchang@po.iams.sinica.edu.tw.
[†] Institute of Atomic and Molecular Sciences.
[‡] Department of Chemistry.
[§] State Key Laboratory of Molecular Reaction Dynamics.

10.1021/jp004103f CCC: $20.00 © 2001 American Chemical Society
Published on Web 09/11/2001

Ner and Speller[21] have sought to determine the number of the first hydration shell of H^+FA based on thermochemical criteria derived from hydration enthalpy measurements for a wide variety of cluster ions. Conclusive determination of this number, however, could not be made due to the lack of a distinct discontinuous drop in the hydration energy of $H^+FA(H_2O)_n$ with n. The result, similarly found for $NH_4^+(H_2O)_n$,[22] arises primarily from the existence of more than one comparably stable isomer that obscures the effect of shell filling.

We have recently devoted ourselves to obtaining the infrared spectra of protonated formamide clusters produced by a supersonic expansion using a vibrational predissociation ion trap spectrometer. With aid of ab initio calculations, the obtained spectra provide relevant structural information about the nature of the hydration of a protonated formamide cation in liquid water. In an earlier report,[16] we presented experimental evidence which confirms the O-protonation of formamide from a careful comparison of the experimental spectra with the theoretically predicted stick diagrams of both $NH_4^+(FA)_3$ and $H^+(FA)_3$. In this work, we focus on the study of $H^+FA(H_2O)_{1-4}$ in an effort to reveal how an O-protonated formamide cation is hydrogen-bonded by water sequentially in the gas phase. We extended previous theoretical investigations,[6,7,13] which are mainly limited to $n = 1$ of $H^+FA(H_2O)_n$, to larger clusters and closely examined their lowest-energy isomers based on density functional theory calculations. We further performed vibrational spectroscopic measurements on size-selected $H^+FA(H_2O)_{3,4}$ clusters using a vibrational predissociation technique to verify the calculations. Moreover, we carried out both measurements and calculations of $H^+(FA)_3H_2O$ to search for shell-filled structures. It is concluded from this combined investigation that a picture with a mobile proton within the clusters is more realistic than the normally accepted model that the proton is firmly attached to the formamide molecule.

Methods

Experimental measurements of the vibrational spectra of protonated formamide−water clusters were performed with use of a vibrational predissociation spectrometer in conjunction with a pulsed infrared laser, described in detail elsewhere.[22] Briefly, we synthesized the mixed cluster ions by a supersonic expansion of corona-discharged $HC(O)NH_2/H_2O$ vapor seeded in pure H_2 at a backing pressure of roughly 100 Torr behind a room-temperature nozzle. A 60° sector magnet first selected the cluster ions of interest $[H^+FA(H_2O)_n]$, which were then stored in an octopole ion trap for both temperature and spectroscopic measurements. Inside the trap, an infrared laser promoted the cluster ions to the first vibrationally excited states. Water loss from the vibrational excitation and the resulting fragmentation, $H^+FA(H_2O)_n + h\nu \rightarrow H^+FA(H_2O)_{n-1} + H_2O$, was monitored by a quadrupole mass filter. The fragment ion signals $[H^+FA(H_2O)_{n-1}]$ were recorded as a function of the excitation laser wavelength to obtain the infrared action spectra. The typical internal temperature of these clusters is 170 K.[16,22]

A prior study[16] inadvertently found that NH_4^+ ions were produced simultaneously with the protonated formamide cations due to metastable fragmentation of internally hot H^+FA species. These ions (NH_4^+) facilely formed clusters with FA and H_2O, giving rise to $H^+FA(NH_3)(H_2O)_{n-1}$, which differs from $H^+FA(H_2O)_n$ by only one M/e unit. They must be sufficiently separated to avert cross contamination. However, in this experiment, to obtain a sufficient number of ions for spectroscopic measurements, we intentionally lowered the resolution of the magnet mass spectrometer to $M/\Delta M \sim 150$ to increase ion intensity. This limits the range of our exploration to clusters with a size of $n < 5$.

TABLE 1: Comparison of the DFT-calculated Total Interaction Energies (kcal/mol) of the Clustering, $H^+[HC(O)NH_2] + nH_2O \rightarrow H^+[HC(O)NH_2](H_2O)_n$, with Experimental Measurements

	calcd[a]				exptl[b]	
isomers[c]	$-\Delta E_n$[d]	$-\Delta H_n^{298}$	$-\Delta G_n^{298}$	$-\Delta G_n^{170}$	$-\Delta H_n^\circ$	$-\Delta G_n^\circ$
FAW1I	21.0	21.5	12.9	16.6	21.2	13.2
FAW1II	20.8[e]					
FAW2I	34.3	35.3	18.6	25.8	35.2	20.3
FAW2II	33.8	34.6	18.2	25.2		
FAW2III	33.2	33.8	17.9	24.7		
FAW2IV	27.9	28.8	11.8	19.1		
FAW3I	46.6	47.9	23.6	34.1	47.0	25.8
FAW3II	45.6	46.8	22.5	32.9		
FAW3III	44.8	45.9	22.0	32.3		
FAW3IV	44.1	44.8	21.6	31.5		
FAW4I	56.2	57.8	26.2	39.8	56.7	29.5
FAW4II	56.8	58.0	26.7	40.1		
FAW4III	55.8	56.9	26.1	39.3		
FAW4IV	54.7	55.8	24.5	38.0		
FAW4V	54.7	57.3	21.8	37.0		

[a] Except that of isomer **FAW1II**, all the calculated energies are given with respect to the trans form of the O-protonated H^+FA. [b] Reference 21. [c] Structures illustrated in Figures 1 and 2. [d] Zero-point vibrational energies corrected. [e] With respect to the cis form of the O-protonated H^+FA.

Parallel with experiments, density functional theory (DFT) calculations were carried out using the commercial GAUSSIAN 98 package[23] at the B3LYP/6-31+G* level of computation. Geometries of the clusters were optimized by analytical gradients without imposing any symmetry constraints and harmonic frequencies were obtained from analytical second derivatives. The calculations supplied both harmonic vibrational frequencies and infrared absorption intensities of various structural isomers to be compared directly with our observations. To establish a better agreement between calculations and measurements, a larger basis set (aug-cc-pVTZ) was used to calculate the binding energies (cf. Table 1), on the basis of the optimized geometries and zero-point vibrational energies produced by B3LYP/6-31+G*.

In scaling the calculated frequencies to compare with observations, we found that the use of a single scaling factor does not suffice to reproduce simultaneously the experimentally observed free-NH and −OH stretching frequencies. A single scaling factor ($\times 0.973$) was chosen for the OH stretches, according to our previous studies of neutral and charged water clusters.[25] Application of this factor to the NHs of FA, however, resulted in significant overestimation (by ~ 35 cm^{-1}) of the free-NH stretching frequencies of both neutral and protonated formamide molecules.[16] The overestimation, presumably, results from the difference in vibrational anharmonicity between these two types of stretches and, hence, two scaling factors ($\times 0.973$ and $\times 0.963$) were used separately for the vibrational frequencies of OH and NH, respectively, throughout this work.

Results and Analysis

Following our previous designation for the NH stretching modes of formamide,[16] four symbols are used to classify the NH stretching motions according to how intermolecular hydrogen bonds are formed within the $H^+FA(H_2O)_n$ clusters. They are the asymmetric free-NH (denoted as a-NH_2), symmetric free-

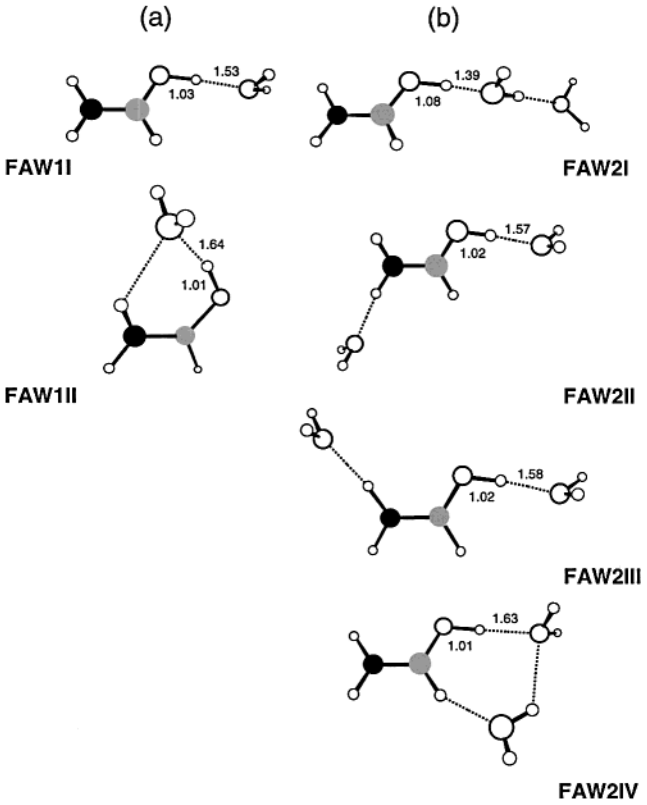

Figure 1. DFT-optimized structures of (a) $H^+[HC(O)NH_2]H_2O$ and (b) $H^+[HC(O)NH_2](H_2O)_2$. The C, N, O, and H atoms are denoted by shaded spheres, solid spheres, large open spheres, and small open spheres, respectively. The given bond lengths are all in the unit of angstrom.

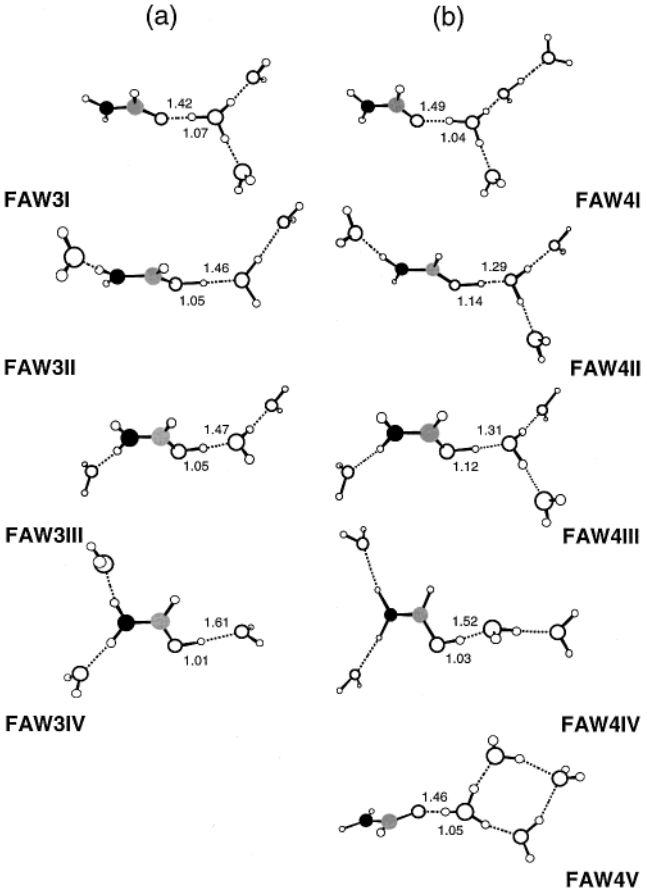

Figure 2. DFT-optimized structures of (a) $H^+[HC(O)NH_2](H_2O)_3$ and (b) $H^+[HC(O)NH_2](H_2O)_4$. The C, N, O, and H atoms are denoted by shaded spheres, solid spheres, large open spheres, and small open spheres, respectively. The given bond lengths are all in the unit of angstrom.

NH (denoted as s-NH_2), non-hydrogen-bonded free-NH (denoted as f-NH), and hydrogen-bonded-NH (denoted as b-NH) stretches. Similar notations are used for the OH stretches of water, denoted as a-OH_2 (asymmetric free-OH), s-OH_2 (symmetric free-OH), f-OH (non-hydrogen-bonded free-OH), and b-OH (hydrogen-bonded-OH), respectively.

A. Theoretical. We begin the theoretical analysis with the $H^+FA(H_2O)$ binary complex, which yields valuable insight into the more complex cluster systems examined in the experiment.[26] Figure 1a displays the isomeric trans- and cis- structures optimized by the DFT calculations for $H^+FA(H_2O)$. The lowest-energy isomer (cf. **FAW1I** in Table 1) consists of an ionic $O-H^+\cdots O$ hydrogen bond with the H_2O aligned in a trans configuration with respect to the C═O double bond of the protonated formamide. This trans arrangement is optimized for its dipole−charge−dipole interactions among the formamide, the proton and the monomeric water. Since the proton affinity of H_2O is 31.3 kcal/mol less than that of FA,[27] **FAW1I** is H^+-FA-centered with an $H^+\cdots OH_2$ hydrogen bond length of 1.53 Å. It is likely that the cis conformer (**FAW1II**) of this cluster can also exist. This isomer, previously identified by Rodriquez et al.[5] in the study of water-assisted tautomerization of a protonated formamide, has two subunits linked by two intermolecular hydrogen bonds with total interaction energy of 20.8 kcal/mol. This energy is comparable to that (21.0 kcal/mol) of **FAW1I** containing a single directional hydrogen bond; however, as the cis conformer of the O-protonated H^+FA itself is less stable than the corresponding trans form by 3.4 kcal/mol,[16] isomer **FAW1II** actually lies above **FAW1I** by 3.6 kcal/mol in terms of total energy. We neglect here the N-protonated forms of $H^+FA(H_2O)$ since they all lie much higher in energy and are less important in this study.[16]

Built on the lowest energy structure of $H^+FA(H_2O)$, namely, **FAW1I**, a number of $H^+FA(H_2O)_2$ isomers can form. Calculations predicted that addition of a foreign water molecule to **FAW1I** can give rise to four low-energy H^+FA-centered isomers. No H_3O^+-centered isomers emerge as formamide has a higher proton affinity than $(H_2O)_2$ by ∼3 kcal/mol.[27,28] These isomers all contain a new hydrogen bond formed between either the OH_2 group or the NH_2 group of $H^+FA(H_2O)$ and the second water molecule. Illustrated in Figure 1b is the lowest-energy isomer of $H^+FA(H_2O)_2$, **FAW2I**, which consists of a water dimer linked to H^+FA in a trans arrangement, a construct strongly favored by the charge-dipole interaction and the hydrogen bond cooperative effect.[29] The second-lowest energy isomer, **FAW2II**, has a water molecule firmly attached to one of the two amino NH bonds with the water dipole aligned nearly parallel to the dipole ($^{\delta-}O-C-N^{\delta+}$) of formamide. This head-to-tail orientation is energetically favored over its counterpart (**FAW2III**) by 0.7 kcal/mol due to stronger charge-dipole interactions exerted in **FAW2II**. The least stable isomer among the four is **FAW2IV**, which is cyclic with a nonlinear $C-H\cdots O$ hydrogen bond.[16,30]

Starting from **FAW2I**−**FAW2III**, four low-lying isomers can be constructed by attachment of one more water molecule to them. It is possible that isomers with the third water molecule residing on the outer solvation shell of the dimeric $FA-H^+-OH_2$ unit can also form. These isomers, however, are all less strongly bound by more than 1 kcal/mol and, hence, are excluded in the present consideration. Out of the four structures depicted in Figure 2a, isomer **FAW3IV**, containing a fairly

symmetrically filled first hydration shell around H^+FA, is *not* lowest in energy. It lies above the global minimum, **FAW3I** (an asymmetric H_3O^+-centered structure), by 2.5 kcal/mol due to the hydrogen bond anticooperative effect,[24] which prohibits both NH bonds to be simultaneously involved in hydrogen bonding. For $H^+FA(H_2O)_n$, a switch over from H^+FA-centered isomers to H_3O^+-centered isomers is expected to occur at $n = 3$, because the proton affinity of the water trimer is ~4 kcal/mol higher than that of formamide.[27,28] The effect is indeed seen for the clustering **FAW2I → FAW3I**, upon which all the three water molecules clump together on one side of formamide, forming a linear $(H_2O)_3$ with the middle water in direct contact with the excess proton. The arrangement results in a movement of the proton toward a site closer to water to overcome the hydrogen bond anticooperative effect that destablizes the linear trimer in the form of $H_2O\cdots H-O-H\cdots OH_2$.

Between the two extreme cases, **FAW3IV** (H^+FA-centered) and **FAW3I** (H_3O^+-centered), there lies two stable H^+FA-centered isomers (**FAW3II** and **FAW3III**), which differ from each other in the orientation of the attached water dipole with respect to the C−N bond of formamide. For the same reasons given above, isomer **FAW3II**, which can be produced either from **FAW2I** or from **FAW2II**, is 0.8 kcal/mol lower in energy than **FAW3III** (Table 1). It is the second-lowest energy isomer of $H^+FA(H_2O)_3$, about 1 kcal/mol less stable than **FAW3I**. According to this calculation, both isomers **FAW3I** and **FAW3II** are expected to be responsible for the spectrum observed experimentally.

Extension of the calculations to $n = 4$ reveals 5 low-energy isomers shown in Figure 2b. These isomers all build on the trans structures of $n = 3$ (Figure 2a), and hence, the relative energy difference between any two consecutive low-lying isomers is small, even smaller than that in $H^+FA(H_2O)_3$. Starting with **FAW3I** (H_3O^+-centered), one finds that an attachment of the water molecule to the amino group can pull the excess proton from water toward the formamide site, due to charge-dipole attractions that overcome the proton affinity difference of ~3 kcal/mol between H^+FA and $(H_2O)_3$. This gives rise to the lowest energy H^+FA-centered isomer **FAW4II**. In contrast, if the fourth water molecule is bound to **FAW3I** by forming one hydrogen bond with one of the water ligands, the charge will be firmly attached to H_3O^+, yielding the second lowest-energy isomer **FAW4I**. The isomer (**FAW4I**) lies above the global minimum (**FAW4II**) by 0.6 kcal/mol but is more stable than its structural counterpart (**FAW4III**) by 0.4 kcal/mol. Analogous to **FAW3IV**, isomer **FAW4IV** containing a filled first hydration shell is about 1.5 kcal/mol higher in energy than **FAW4I**. This energy difference, as compared to the corresponding value of 2.5 kcal/mol for $H^+FA(H_2O)_3$, does seem to diminish as clusters grow. Last, it is worth noting that isomer **FAW4V** (containing an H_3O^+-centered four-membered ring) is equally stable as **FAW4IV**; however, both the enthalpy and entropy effects clearly prevail to favor the open, noncyclic isomers (**FAW4I - FAW4III**) in the supersonic expansions at the cluster temperature of 170 K (Table 1).

As revealed in Table 1, there exists an interesting alternation in relative stability and proton location among the cluster isomers produced by stepwise attachment of each incoming foreign water molecule to $H^+FA(H_2O)_{n-1}$ as n increases from 2 to 4. For $H^+FA(H_2O)_2$, the lowest energy isomer is H^+FA-centered (**FAW2I**). It differs from that of $H^+FA(H_2O)_3$, where the H_3O^+-centered isomer (**FAW3I**) is lowest in energy while the H^+FA-centered one (**FAW3II**) is second lowest. This stability order is further reversed at $n = 4$. It illustrates a unique proton transfer behavior in mixed cluster ions, in which the exact location of the excess proton can vary sensitively with the hydration number, solvation structures, and the proton affinity differences among arranged competing ligands.[31]

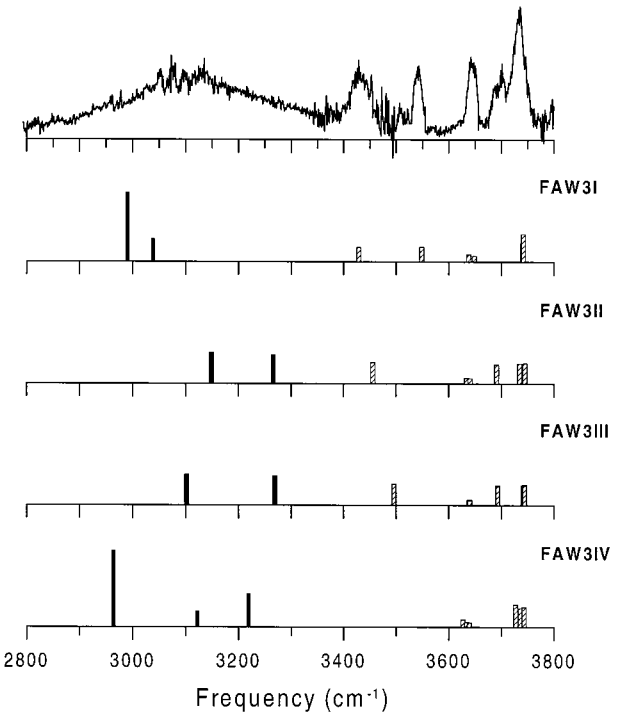

Figure 3. Comparison of the power-normalized vibrational predissociation spectrum of $H^+[HC(O)NH_2](H_2O)_3$ with DFT-calculated stick diagrams of isomers depicted in Figure 2a. The calculated intensities of the free-NH and -OH stretches (slashed bars) have been amplified by a factor of 5 for clearer comparison to those of the bonded-NH and -OH stretches (solid bars). Note that the CH stretches at 2900−3000 cm^{-1} are too weak to be seen in the calculated spectra.

B. Experimental. Experimental spectra were obtained for the cluster ions $H^+FA(H_2O)_3$ and $H^+FA(H_2O)_4$, which have a stepwise dissociation energy ($\Delta H_D°$) of 11.8 and 9.7 kcal/mol (Table 1), respectively. They can be fragmented as a consequence of absorbing a single quantum of infrared radiation (photon energy = 8−11 kcal/mol)[22] at the expense of internal energies (~3 kcal/mol at 170 K).[16] Fragmentation of $H^+FA(H_2O)_{1,2}$ by the same infrared photons (2800−3800 cm^{-1}), however, does not occur effectively since these cluster ions are more strongly bound, with a stepwise dissociation energy of $\Delta H_D° \geq 14.0$ kcal/mol. Their spectra and, hence, the structural information can only be obtained from theoretical calculations.

Figures 3 and 4 depict, respectively, the experimental spectra of $H^+FA(H_2O)_3$ and $H^+FA(H_2O)_4$ in the NH and OH stretching regions over a wide frequency range, 2800−3800 cm^{-1}. Both spectra exhibit a number of distinct absorption bands, but with the $H^+FA(H_2O)_4$ spectrum richer in sharper vibrational features. Four distinct sets of transitions can be clearly identified at 3300−3800 cm^{-1}, and they provide a wealth of information for structural identification of isomers as well as the location and movement of the excess proton in these clusters. One may easily assign these 4 sets of transitions in the spectrum of $H^+FA(H_2O)_4$ on the basis of our previous studies for $NH_4^+(FA)_3$ and $H^+(FA)_3$.[16] They are (1) the f-NH stretch at 3467 cm^{-1} and the b-NH stretch at 3342 cm^{-1}, (2) the a-NH_2 stretch at 3547 cm^{-1} and the s-NH_2 stretch at 3431 cm^{-1}, (3) the f-OH stretch at 3715 cm^{-1} and the b-OH stretch at 3342 cm^{-1}, and (4) the a-OH_2 stretch at 3739 cm^{-1} and the s-OH_2 stretch at 3649 cm^{-1}, respectively. Similarly, 4 sets of transitions [at 3452 (f-NH),

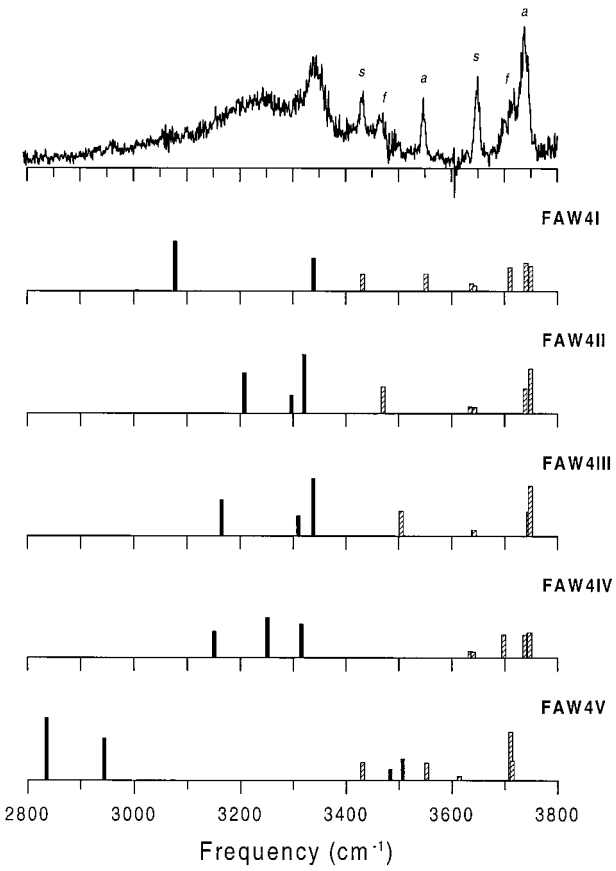

Figure 4. Comparison of the power-normalized vibrational predissociation spectrum of $H^+[HC(O)NH_2](H_2O)_4$ with DFT-calculated stick diagrams of isomers depicted in Figure 2b. The calculated intensities of the free-NH and -OH stretches (slashed bars) have been amplified by a factor of 5 for clearer comparison to those of the bonded-NH and −OH stretches (solid bars). The labels "a", "f", and "s" denote the a-NH_2 (a-OH_2), f-NH (f-OH), and s-NH_2 (s-OH_2) stretches of formamide (water) within the range of 3400 (3600)−3600 (3800) cm^{-1}, respectively. Note that the CH stretches at 2900−3000 cm^{-1} are too weak to be seen in the calculated spectra.

∼3120 (b-NH); 3541 (a-NH_2), 3431 (s-NH_2); 3697 (f-OH), ∼3120 (b-OH); 3733 (a-OH_2), 3644 (s-OH_2) cm^{-1}] can also be found for $H^+FA(H_2O)_3$, although they are substantially broader than those of $n = 4$ (cf. Figure 5a,b). Observing these distinct spectral signatures, we suggest that at least two structural isomers should coexist for each cluster ($n = 3$ and 4) in the supersonic expansion. Such kind of information, in contrast, cannot be provided by the features at the lower frequency region (i.e., 2800−3200 cm^{-1}), where immense band broadening is observed for both the bonded-OH and -NH stretches of $H^+FA(H_2O)_3$ and $H^+FA(H_2O)_4$.

Preliminary structural information can be deduced from the experimental spectra without invoking theoretical calculations. This is particularly the case for cluster isomers producing distinct a-NH_2 and s-NH_2 absorption features in the experimental spectra. For those isomers, to show both the NH_2 stretches, the water molecules must group together sequentially on one side of the formamide, rather than scattering themselves around the H^+FA ion core. This sequential grouping largely increases the possibility of proton transfer from the protonated formamide to water due to the enhancement in proton affinity of the water molecule in direct contact with the excess proton. We have previously estimated[28] that a water dimer has a proton affinity (PA) of 193 kcal/mol, which is higher than that of monomeric water by 27 kcal/mol. Further increasing to 200 kcal/mol is possible for the water molecule situated in the middle of a linear water trimer. This proton affinity exceeds the PA = 196.5 kcal/mol of FA with the oxygen atom acting as the protonation site.[16,27] As a result of the competition for the excess proton between formamide and the water polymers, a transfer of the H^+ from a site close to FA to a site close to water can readily occur at $n = 3$. Hence, isomers containing both types of ion cores (H^+FA and H_3O^+), and/or the intermediates ($FA-H^+-OH_2$), are expected to coexist in the supersonic expansion for each cluster ion.

Comparison of the calculated stick diagrams to the experimental spectrum in Figure 3 corroborates the assignment of the observed vibrational features to **FAW3I** and **FAW3II**, the two lowest-energy isomers of $H^+FA(H_2O)_3$ (Table 1). These two isomers possess distinct vibrational fingerprints that are nearly complementary to each other, and therefore, they can be easily distinguished according to their free-OH and -NH stretching vibrations. One vivid example is that isomer **FAW3I** contains both a-NH_2 and s-NH_2, but not f-NH nor f-OH, whereas isomer **FAW3II** contains both f-OH and f-NH, but not a-NH_2 nor s-NH_2. A combination of the vibrational spectra of these two isomers does reproduce the observed spectrum satisfactorily (cf. Figure 3), supporting the suggestion for the coexistence of H^+-FA-centered and H_3O^+-centered isomers in the supersonic expansion. Compared to **FAW3I** and **FAW3II**, both isomers **FAW3III** and **FAW3IV** are less likely to prevail in the beam because of being relatively higher in energy.

A comparison of the calculated stick diagrams with the experimental spectrum of $H^+FA(H_2O)_4$ in Figure 4, again, allows identification of the two lowest-energy isomers **FAW4I** and **FAW4II**, each also having distinct vibrational signatures complementary to each other for both the free-OH and NH stretches in the spectra. For instance, isomer **FAW4II** contains only f-NH, but not a-NH_2, s-NH_2, nor f-OH, whereas isomer **FAW4I** contains not only f-OH but also both a-NH_2 and s-NH_2. A coupled observation of these vibrational signatures, as displayed in Figure 4, proves the coexistence of both H^+FA-centered and H_3O^+-centered isomers of $H^+FA(H_2O)_4$ in the supersonic expansion. Similar to **FAW3III**, isomer **FAW4III** failed to be identified in the expansion, because it is not only higher in energy but also its f-NH frequency matches poorly with observations. Detailed assignments of the observed absorption bands, a list of the corresponding bandwidths, along with the calculated frequencies of $H^+FA(H_2O)_3$ and $H^+FA(H_2O)_4$ isomers are given in Table 2.

Discussion

A. The Proton Pulling Effect. Indicated in Figures 1 and 2 are the lengths of the two $O-H^+$ bonds involving the excess proton in each $H^+FA(H_2O)_{1-4}$. The proton in these clusters can either be localized at a site closer to formamide (H^+FA-centered), at a site closer to water (H_3O^+-centered), or somewhere between them. We may understand this intriguing behavior in terms of a proton pulling effect derived from a competition for the excess proton between the subunits (FA and H_2O) residing on either side of the H^+ in the clusters.[28,31,32] Following Ciobanu et al.,[33] a proton localization (or delocalization) parameter f can be used to describe this proton pulling effect quantitatively,

$$f = (r_f - r_w)/(r_f + r_w) \quad (1)$$

where r_f and r_w are the lengths of the $O-H^+$ bonds involving the excess proton for formamide and water, respectively. The sum ($r_f + r_w$) is essentially equal to the interoxygen distance

TABLE 2: Frequencies (cm^{-1}) and Assignments of Observed NH and OH Stretching Absorption Bands of $H^+[HC(O)NH_2](H_2O)_{3,4}$

observed frequency	fwhm[a]	calcd frequency[b]	isomers[c]	assignments
3733	22	3740, 3742, 3735, 3745	**FAW3I, FAW3II**	a-OH_2 of 1° or 2° H_2O
3697	23	3692	**FAW3II**	f-OH of 1° H_2O
3644	15	3638, 3639, 3634, 3641	**FAW3I, FAW3II**	s-OH_2 of 1° or 2° H_2O
3541	13	3549	**FAW3I**	a-NH_2 of FA
3452[d]	10	3457	**FAW3II**	f-NH of H^+FA
3431[d]	33	3429	**FAW3I**	s-NH_2 of FA
3120	240	3266	**FAW3II**	b-OH of 1° H_2O
		3149	**FAW3II**	b-NH of H^+FA
		2990, 3038	**FAW3I**	b-OH of H_3O^+
3739	13	3741, 3750, 3739, 3749	**FAW4I, FAW4II**	a-OH_2 of 1° or 2° H_2O
3715	13	3711	**FAW4I**	f-OH of 1° H_2O
3649	8	3637, 3644, 3635, 3643	**FAW4I, FAW4II**	s-OH_2 of 1° or 2° H_2O
3547	7	3552	**FAW4I**	a-NH_2 of FA
3467	15	3471	**FAW4II**	f-NH of H^+FA
3431	13	3432	**FAW4I**	s-NH_2 of FA
3342	29	3339	**FAW4I**	b-OH of 1° H_2O
		3321	**FAW4II**	b-NH of H^+FA
3240[d]	130	3208, 3297	**FAW4II**	b-OH of H_3O^+
3073[d]	90	3078	**FAW4I**	b-OH of H_3O^+

[a] Full width at half-maximum. [b] Frequencies scaled by ×0.963 for NH and ×0.973 for OH stretches. [c] Structures illustrated in Figures 1 and 2. [d] Obtained by band deconvolution.

TABLE 3: Dependence of the Proton Localization Parameter *f* on Cluster Size and Cluster Structure

	$f \equiv (r_f - r_w)/(r_f + r_w)$[a]			
isomers[b]	$n = 1$	$n = 2$	$n = 3$	$n = 4$
FAWnI	−0.195	−0.125	+0.142	+0.175
FAWnII		−0.215	−0.168	−0.062
FAWnIII		−0.216	−0.165	−0.079
FAWnIV			−0.231	−0.191
FAWnV				+0.164

[a] Defined by eq 2 in text. [b] Structures illustrated in Figures 1 and 2.

R_{OO}, since the $O_f\cdots H^+\cdots O_w$ hydrogen bonds in these clusters are all nearly linear. By this definition, the proton localization parameter can vary from $f < 0$, with the proton localized at a site closer to the formamide, to $f > 0$, with the proton localized at a site closer to water. In the case that $r_f = r_w$ and $f = 0$, the proton is shared equally by these two subunits. Table 3 provides a list of *f*'s calculated from eq 2 for clusters **FAW1I** to **FAW4IV**. The values vary over a wide range from $f = -0.2$ to $f = +0.2$, revealing a dynamic nature of the excess proton along the $O_f\cdots H^+\cdots O_w$ hydrogen bond in water-containing clusters. Analogous to the effect previously observed for $H^+[(CH_3)_2O](H_2O)_n$,[28] the O_f-H^+ bond in isomers **FAWnI** is systematically elongated from $r_f = 1.03$ Å to $r_f = 1.49$ Å, as increasingly more water molecules keep on clustering on one side of the formamide of $H^+FA(H_2O)_n$ ($n = 1 \rightarrow 4$ in Figures 1 and 2). The *f* value accordingly increases (from left to right in Table 3) as the numerator $(r_f - r_w)$ in eq 2 becomes larger.

Of clusters $H^+FA(H_2O)_{1-4}$, the isomers with the smallest absolute value of *f* are **FAW4II** and **FAW4III**, with $f = -0.062$ and −0.079, respectively. They both have a calculated bond length difference $(r_f - r_w)$ of less than 0.2 Å, about one-tenth of the interoxygen distance, $R_{OO} \approx r_f + r_w \approx 2.42$ Å. Figure 6 displays the result of a scan of the potential energy surface along the proton-transfer coordinate $(r_f - r_w)$ of **FAW4II**, obtained at the B3LYP/6-31+G* level of computation. A shallow potential emerges, with a well depth varying by less than 0.2 kcal/mol over the bond length range of $r_f - r_w = -0.23$ Å to +0.17 Å or, equivalently, $r_f = 1.1-1.3$ Å. As in the case of $H^+[(CH_3)_2O](H_2O)_2$ previously studied,[28] the proton in it can undergo a large amplitude motion (or proton shuffling) between O_f and O_w when experiencing the zero-point vibrational effect

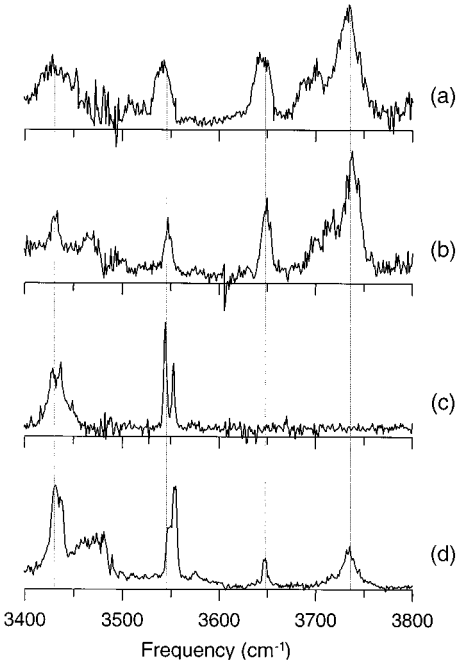

Figure 5. Enlarged view of the power-normalized vibrational predissociation spectra of (a) $H^+[HC(O)NH_2](H_2O)_3$, (b) $H^+[HC(O)NH_2](H_2O)_4$, (c) $H^+[HC(O)NH_2]_3$, and (d) $H^+[HC(O)NH_2]_3H_2O$ in the free-NH and −OH stretching region. The poorer signal-to-noise ratios at ~3480 cm^{-1} derive from lower output power density of the infrared laser produced by difference frequency mixing in a $LiNbO_3$ crystal (ref 22). Four vertical lines are given as a reference for easier comparison of the band positions of the s-NH_2, *a*-NH_2, s-OH_2, and *a*-OH_2 stretches (from left to right) of these four clusters.

which tends to delocalize the extra charge between these two subunits, H_2O-FA and $(H_2O)_3$. Such proton shuffling conceivably may result in modulation of the vibrational frequencies and, consequently, broaden the absorption bands of both the bonded-OH and −NH stretches of the subunits in direct contact with the excess proton.[28]

In searching for experimental evidence for the proton movement in these clusters, our attention was turned to the spectral frequency shifts of the free-NH stretches in Table 2. Figure 5a,b compare in detail the spectra of $H^+FA(H_2O)_3$ and $H^+FA(H_2O)_4$

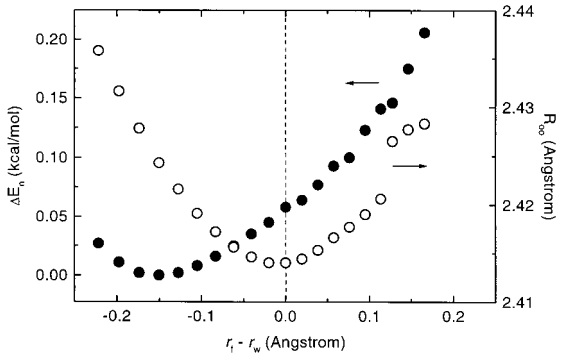

Figure 6. Variation of the potential energies (solid spheres) and interoxygen distances (open spheres) of **FAW4II** along the proton-transfer coordinate ($r_f - r_w$), defined as the O−H$^+$ bond length difference between formamide and the water molecule in direct contact with the excess proton (see text for details). Note that $R_{OO} \approx r_f + r_w$, because the O···H$^+$···O hydrogen bond is essentially linear.

for their free-NH stretches. Slight band shifting toward the higher frequency side (by +6 cm^{-1}) is detected for a-NH$_2$ as cluster size increases from $n = 3$ to $n = 4$. Such a frequency shift is consistent with a picture, in which the excess proton is perturbed more by the grouped water in **FAW4I** ($f = +0.175$) than in **FAW3I** ($f = +0.142$), giving rise to an increase in bond length difference ($r_f - r_w$) of 0.09 Å at a larger n. More prominent frequency shifting can be found for the f-NH resonance at ∼3450 cm^{-1}. While the absorption band of this stretch merges with that of s-NH$_2$ at $n = 3$, producing a broad feature centered at ∼3440 cm^{-1}, a corresponding frequency shift of +15 cm^{-1} can be estimated, obtained by Gaussian multipeak fitting. The result, again, is understood as a consequence of further increment of the proton affinity of the water molecule in direct contact with the H$^+$ as the cluster grows from **FAW3II** ($f = -0.168$) to **FAW4II** ($f = -0.062$), and an increase in bond length difference of 0.26 Å from $n = 3$ to $n = 4$.

In prior studies,[28,31,32] we demonstrated that the excess proton in protonated water-containing clusters is mobile. The exact location of the proton depends sensitively on the structure and solvation number of the clusters. The effect is particularly manifested in H$^+$(H$_2$O)$_{2m}$, where the local environment of the excess proton decides whether the central ion should be either H$_5$O$_2^+$-like or H$_3$O$^+$-like.[33,34] Employing ab initio molecular dynamics calculations, Parrinello and co-workers[34] have explored the dynamics of proton transfer in large protonated water clusters. Aiming at unraveling the nature of proton migration in liquid bulk water, they concluded that the excess proton in water can be considered part of a "low-barrier hydrogen bond" and the rate of the H$^+$ migration is governed by thermally induced breaking of hydrogen bonds in the second solvation shell. Together with their calculations, the present results lead us to expect that the dynamics of proton transfer may play an important role in the process of acid-catalyzed hydrolysis of formamide, or even polypeptides, in aqueous solutions. Such proton transfer effects, to our knowledge, have not yet been properly taken into account in prior analysis of FA hydrolysis and certainly deserve a close examination in future calculations.

The biological relevance of formamide as a model of a peptide link motivates us to search further for cluster isomers that are possibly the intermediates in the process of acid-catalyzed formamide hydrolysis. Bader and co-workers[7] first suggested the existence of an intermediate, with the oxygen atom of a water molecule bound to the carbon atom of the O-protonated formamide, for an H$^+$FA-H$_2$O binary complex. Antoczak et al.[9] extended the calculations to H$^+$FA(H$_2$O)$_3$ and found that water

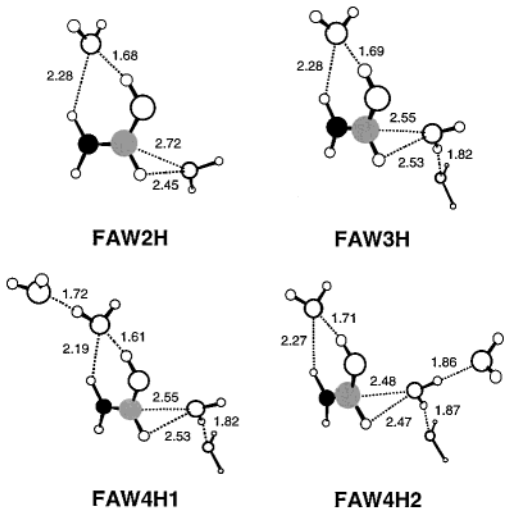

Figure 7. DFT-optimized structures of the reaction intermediates in acid-catalyzed hydrolysis of formamide for H$^+$[HC(O)NH$_2$](H$_2$O)$_{2-4}$. The C, N, O, and H atoms are denoted by shaded spheres, solid spheres, large open spheres, and small open spheres, respectively, and the given bond lengths are all in the unit of angstrom. Provided by the B3LYP/aug-cc-pVTZ level of calculation, the total interaction energies of these reaction intermediates (with respect to the cis form of the O-protonated H$^+$FA) are $\Delta E_n = -28.2$, -35.7, -47.6, and -42.0 kcal/mol for clusters **FAW2H**, **FAW3H**, **FAW4H1**, and **FAW4H2**, respectively.

can promote the hydrolysis of formamide by forming a more stable intermediate and, simultaneously, lowering the barrier height of the hydrolysis. We have also attempted to scan the potential energy surfaces of H$^+$FA(H$_2$O)$_{2-4}$ and searched for the intermediates (stable isomers) suggested by these authors using the B3LYP/aug-cc-pVTZ level of computation. Four stable intermediates, each containing an H$_2$O···C contact (Figure 7), were identified during the course of this calculation. As one may have expected, they all lie much higher (∼10 kcal/mol) in energy than the lowest energy isomers experimentally observed in this work. While no indication was found for the narrowing of this energy gap at a larger n (cf. the caption of Figure 7), the O···C bond length does show a propensity to decrease as n increases (see Figure 7 for details).[36]

B. Filling of the First Hydration Shell. Guided by theoretical calculations, the present study attempted to acquire direct experimental evidence for the existence of H$^+$FA-centered isomers containing a filled first hydration shell in clusters H$^+$-FA(H$_2$O)$_{3,4}$. Unfortunately, no concrete evidence was found for **FAW3IV** and **FAW4IV** in the corona-discharged supersonic expansion. Two factors may be responsible for this failure in observation. First, the shell-filled isomers lack distinguishable vibrational features (such as the free NH stretches), which makes their identification difficult. Second, the isomers, having both amino NH groups hydrogen-bonded to the water molecules, are not lowest in energy due to the hydrogen bond anticooperative effect.[24] Hence, they may not be produced in sufficient abundance for spectroscopic detection using infrared photons. In view of the importance of hydration in acid-catalyzed amide hydrolysis, we deduce the information of how the first solvation shell of H$^+$FA is filled from the DFT calculation, since the calculation has been able to reproduce several salient spectral signatures of the lowest-energy isomers of H$^+$FA(H$_2$O)$_{3,4}$ in earlier sections.

Table 1 summarizes the relative stability of H$^+$FA(H$_2$O)$_{1-4}$ isomers. The shell-filled, H$^+$FA-centered isomers (**FAW3IV** and **FAW4IV**) are both significantly higher (∼2 kcal/mol) in energy than their H$_3$O$^+$-centered counterparts, even though both ion

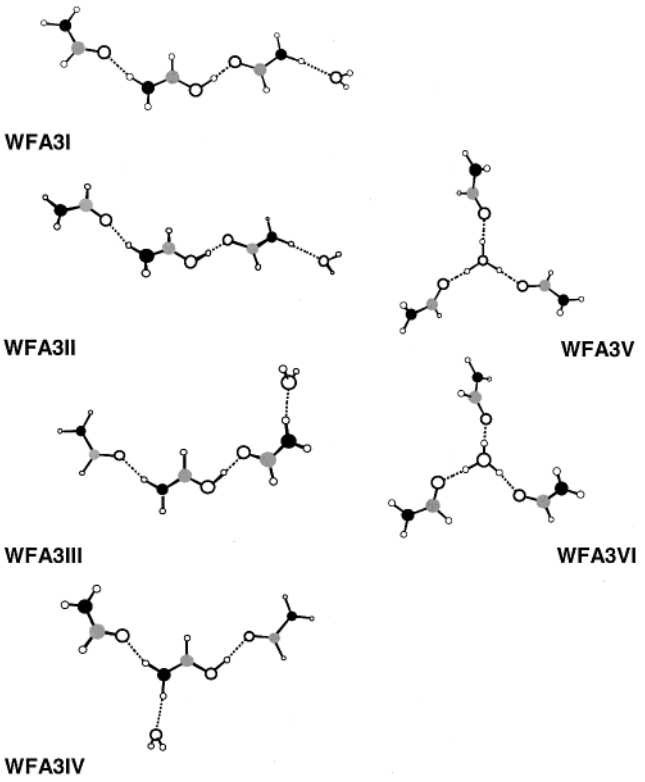

Figure 8. DFT-optimized structures of $H^+[HC(O)NH_2]_3H_2O$. The C, N, O, and H atoms are denoted by shaded spheres, solid spheres, large open spheres, and small open spheres, respectively.

cores are capable of accepting the same number of ligand molecules to form the first solvation shell. One may easily comprehend this result from Mulliken charge analysis.[35] For the O-protonated H^+FA, the analysis reveals that the NH_2 group carries a charge close to $+0.47e$ (e = electron charge), compared to $-0.55e$ of the OH group. This charge distribution markedly differs from that of H_3O^+, which contains three geometrically equivalent OH moieties. Solvation of the O-protonated formamide cation can, therefore, bias toward the OH group and the water molecules are facilitated to cluster on one side of H^+FA and, eventually, form an H_3O^+ ion core.

Instructive comparison of the hydration asymmetry and isomerism can further be made between H^+FA and NH_4^+.[22] These two cluster systems, $[H^+FA(H_2O)_n$ and $NH_4^+(H_2O)_n]$, share the same property that initiation of the second shell starts before the first hydration shell is completely filled. As a result, no distinct shell filling effects were observed in mass spectrometric measurements,[21] whereas a wider variety of structural isomers are found spectroscopically.[22]

To provide experimental evidence for the filling of the first hydration shell around H^+FA, we carried out an additional measurement on $H^+(FA)_3H_2O$ at the same cluster temperature (170 K). The measurement follows our previous studies on $H^+(FA)_3NH_3$ (ref 16) and is stimulated by the idea that if one can sufficiently lower the number of water molecules, which tend to group together, a filled first hydration shell is likely to form around the H^+FA cation. For $H^+(FA)_3H_2O$, predominantly H^+FA-centered isomers should exist and water, having a lower proton affinity than FA, is expected to behave like a ligand hydrogen-bonded to a linear protonated formamide trimer.[16] In this experiment, water loss was monitored to obtain the vibrational predissociation spectrum and DFT calculations were performed to search for any possible shell-filled stable isomers of $H^+(FA)_3H_2O$.

TABLE 4: DFT-Calculated Total Interaction Energies (kcal/mol) of the Clustering, $H^+[HC(O)NH_2] + 2[HC(O)NH_2] + H_2O \rightarrow H^+[HC(O)NH_2]_3(H_2O)$

	calcd[a]			
isomers[b]	$-\Delta E_n$[c]	$-\Delta H_n^{298}$	$-\Delta G_n^{298}$	$-\Delta G_n^{170}$
WFA3I	60.9	60.9	35.3	46.3
WFA3II	60.3	60.1	35.0	45.8
WFA3III	60.0	59.9	34.7	45.5
WFA3IV	59.9	59.6	34.9	45.5
WFA3V	61.7	62.1	35.9	47.2
WFA3VI	60.2	60.7	34.4	45.7

[a] With respect to the trans form of the O-protonated H^+FA. [b] Structures illustrated in Figure 8. [c] Zero-point vibrational energies corrected.

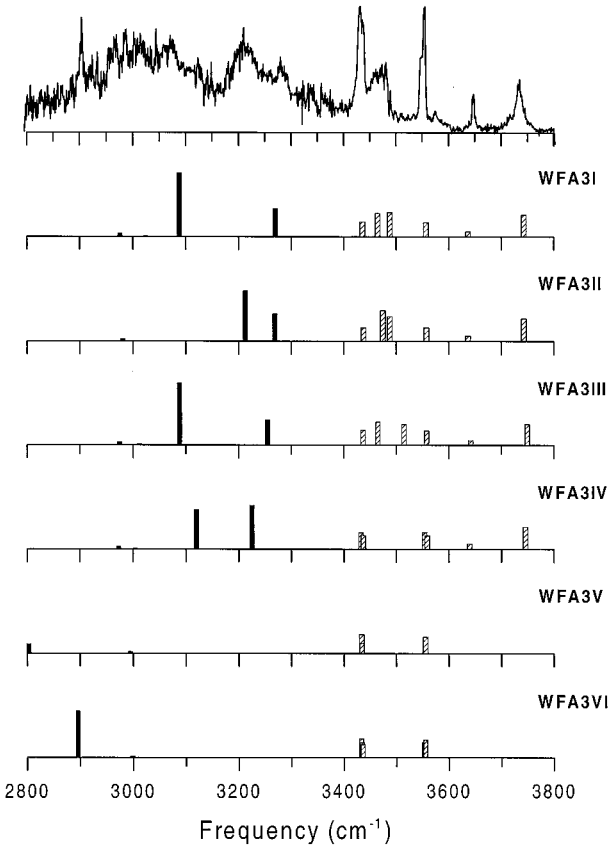

Figure 9. Comparison of the power-normalized vibrational predissociation spectrum of $H^+[HC(O)NH_2]_3H_2O$ with DFT-calculated stick diagrams of isomers **WFA3I**−**WFA3VI**. The calculated intensities of the free-NH and -OH stretches (slashed bars) have been amplified by a factor of 5 for clearer comparison to those of the bonded-NH and -OH stretches (solid bars).

Figure 8 depicts the structures of six low-lying isomers of $H^+(FA)_3H_2O$. They are the more strongly bound isomers among 14 structures we have considered. Similar to the findings for $H^+FA(H_2O)_n$, isomers containing either an H^+FA ion core (**WFA3I**−**WFA3IV**) or an H_3O^+ ion core (**WFA3V** and **WFA3VI**) can coexist. The lowest-energy isomer **WFA3V** is H_3O^+-centered (Table 4), and it differs from its counterpart **WFA3VI** in the orientation of three formamide ligand molecules with respect to each other, resulting in an energy difference of 1.5 kcal/mol. Note that, among these six isomers selectively depicted in Figure 8, **WFA3IV** is the only H^+FA-centered isomer consisting of a filled first solvation shell. The shell, composed of one water and two formamide molecules, is to be identified by the present experiment.

TABLE 5: Frequencies (cm^{-1}) and Assignments of Observed NH and OH Stretching Absorption Bands of $H^+[HC(O)NH_2]_3(H_2O)$

observed frequency	fwhm[a]	calcd frequency[b]	isomers[c]	assignments
3734	17	3743, 3743, 3746	**WFA3I, WFA3II, WFA3IV**	a-OH_2 of H_2O
3647	5	3637, 3637, 3640	**WFA3I, WFA3II, WFA3IV**	s-OH_2 of H_2O
3554[d]	4	3558, 3558, 3559	**WFA3I, WFA3II, WFA3IV**	a-NH_2 of FA
3548[d]	5	3554	**WFA3IV**	a-NH_2 of FA
3480[d]	6	3488, 3488	**WFA3I, WFA3II**	f-NH of FA
3465[d]	13	3465, 3475	**WFA3I, WFA3II**	f-NH of H^+FA
3437	9	3436, 3438, 3437	**WFA3I, WFA3II, WFA3IV**	s-NH_2 of FA
3431	11	3433	**WFA3IV**	s-NH_2 of FA
3277[d]	31	3271, 3256	**WFA3I, WFA3II**	b-NH of FA
3212[d]	42	3213, 3224	**WFA3II, WFA3IV**	b-NH of H^+FA
3074[d]	34	3088, 3120	**WFA3I,WFA3IV**	b-NH of H^+FA

[a] Full width at half-maximum. [b] Frequencies scaled by $\times 0.963$ for NH and $\times 0.973$ for OH stretches. [c] Structures of the isomers are illustrated in Figure 8. [d] Obtained by band deconvolution.

Figure 9 compares the experimental spectrum of $H^+(FA)_3H_2O$ to the DFT-calculated stick diagrams of isomers **WFA3I**−**WFA3VI**. In the spectrum, two features appear in the frequency range of 3600−3800 cm^{-1}, and they belong to the a-OH_2 (3734 cm^{-1}) and s-OH_2 (3647 cm^{-1}) stretches of neutral water molecules. Their appearance immediately suggests the possibility for the existence of isomers **WFA3I**−**WFA3IV** in the supersonic expansion, since these isomers all contain a neutral water molecule situated at the outer solvation shell of the H^+-FA ion core. Analogous to the free-OH, the free-NH stretches also have features standing out at 3400−3600 cm^{-1}, belonging to the a-NH_2 and s-NH_2 stretches of the neutral FA molecules acting as single-proton acceptors in the outer solvation shell of either the H^+FA or the H_3O^+ ion core. A closer inspection of these two NH stretching features (Figure 5d) reveals that each one of them is actually composed of two peaks, resembling the doublet observed for $H^+(FA)_3$ (cf. Figure 5c).[16] It indicates that there exist more than two different bonding sites for neutral FA in this cluster. Of the 6 isomers presently considered, only **WFA3IV** displays such a characteristic vibrational signature. The calculated frequency difference between the free-NH stretches of these two neutral FA molecules in **WFA3IV** is ∼5 cm^{-1} (Figure 9 and Table 5), which remarkably well reproduces the observed splittings of ∼6 cm^{-1}, obtained by band deconvolution of the experimental spectrum. This remarkable match represents a successful identification for the existence of an O-protonated formamide cluster, containing a filled first solvation shell of H^+FA, in the supersonic expansion.

In addition to **WFA3IV**, we also identify isomers **WFA3I** and **WFA3II** from their distinct free-NH vibrations. Fingerprints of these isomers, which are close in energy within 0.6 kcal/mol, are the two closely spaced f-NH stretching bands at ∼3470 cm^{-1} arising from the two FA molecules situated in the middle of the linear hydrogen-bonded chains (Figure 9). One may rule out the possibility for the existence of **WFA3III** in the beam by noting that one of the calculated f-NH stretching frequencies (3465 and 3515 cm^{-1}) of this isomer significantly deviates from that recorded at 3465 and 3480 cm^{-1} for **WFA3I** and **WFA3II** by 35 cm^{-1}. Resembling that of **FAW4IV**, identification for the existence of the lower energy isomers (**WFA3V** and **WFA3VI**) in the supersonic expansion has not been successful due to the lack of distinguishable vibrational features for observations. Detailed assignments of these vibrational features, along with the comparison between calculations and observations, are given in Table 5.

Conclusions

Stimulated by our interest in physical chemistry of biological molecules in aqueous solutions,[16] we have systematically investigated the structures, energetics, isomerization, and dynamics of protonated formamide water clusters in the gas phase, which serves as a unique environment for detailed study of ion hydration processes. Useful information, such as the sites of protonation and hydration, along with the isomeric structures of hydration shells, was deduced from extensive density functional theory calculations for $H^+FA(H_2O)_{1-4}$ and infrared spectroscopic measurements for $H^+FA(H_2O)_{3,4}$. The deduced information is consistent with our previous experience on the similar but less complex systems, $NH_4^+(H_2O)_n$ (ref 22) and $H^+(H_2O)_n$.[32] For $H^+FA(H_2O)_{3,4}$, it is found that multiple isomers, which typically differ in energy by ∼1 kcal/mol, can be produced simultaneously by the corona-discharged supersonic expansion. Cluster isomers, which contain two distinct types of ion core (H^+FA or H_3O^+), coexist; whichever prevails in the expansion depends sensitively on the hydration structure and also on the size of these cluster isomers. Finally, we demonstrated that the shell-filled isomer of $H^+(FA)_3H_2O$ can be synthesized by the expansion as well.

The data collected in this work may provide useful insight into the nature of hydration and protonation of secondary amides, such as *N*-methylformamide and *N*-methylacetamide, in the gas phase.[37] It may also shed light on the hydration of peptides in enzyme cavities where bulk solvation is precluded and the embedded ions are only partially hydrated by a few water molecules.[38] Such information can be critical for a thorough understanding of folding, refolding and hydration of gas-phase proteins, which have primarily been investigated using mass spectrometric methods.[39−41] It is expected that the present examination, combining mass spectrometry, infrared spectroscopy and ab initio calculations, can help clarify the structure of the water network around the protonated formamide cation in liquid water. Ultimately, it can lead to detailed elucidation of the mechanism of enzymatic peptide cleavage,[42] a subject that has been a long-standing interest of biochemists.

Acknowledgment. We thank the Academia Sinica and the National Science Council (Grant No. NSC 89-2113-M-001-081) of Taiwan, the Republic of China, for financial support. We are also indebted to Prof. Y. T. Lee for many helpful discussions.

Supporting Information Available: Detailed geometry information concerning the bond angles and lengths of all the isomers considered in text is viewable with the program Chem 3-D. This material is available free of charge via the Internet at http://pubs.acs.org.

References and Notes

(1) For example, see: Cui, Q.; Karplus, M. *J. Chem. Phys.* **2000**, *112*, 1133.

(2) Wang, X.-C.; Nichols, J.; Feyereisen, M.; Gutowski, M.; Boatz, J.; Haymet, A. D. J.; Simons, J. *J. Phys. Chem.* **1991**, *95*, 10419.
(3) Adamo, C.; Cossi, M.; Barone, V. *J. Comput. Chem.* **1997**, *18*, 1993.
(4) Guo, J.-X.; Ho, J.-J. *J. Phys. Chem. A* **1999**, *103*, 6433.
(5) Rodriquez, C. F.; Cunje, A.; Shoeib, T.; Chu, I. K.; Hopkinson, A. C.; Siu, K. W. M. *J. Phys. Chem. A* **2000**, *104*, 5023.
(6) Lowry, T. H.; Richardson, K. S. *Mechanism and Theory in Organic Chemistry*; 3rd ed.; Harper & Row: New York, 1987.
(7) Laidig, K. E.; Bader, R. F. W. *J. Am. Chem. Soc.* **1991**, *113*, 6312. Krug, J. P.; Popelier, P. L. A.; Bader, R. F. W. *J. Phys. Chem.* **1992**, *96*, 7604.
(8) Lin, H.-Y.; Ridge, D. P.; Uggerud, E.; Vulpius, T. *J. Am. Chem. Soc.* **1994**, *116*, 2996.
(9) Antoczak, S.; Ruiz-Lopez, M. F.; Rivail, J. L. *J. Am. Chem. Soc.* **1994**, *116*, 3912.
(10) Casteiger, J.; Hondelmann, U.; Rose, P.; Witzenbichler, W. *J. Chem. Soc., Perkin Trans. 2* **1995**, 193.
(11) Ou, M.-C.; Chu, S.-Y. *J. Phys. Chem.* **1995**, *99*, 556.
(12) Tortajada, J.; Leon, E.; Mortizur, J.-P.; Luna, A.; MÓ, O.; Yáñez, M. *J. Phys. Chem.* **1995**, *99*, 13890.
(13) Pranata, J.; Davis, G. D. *J. Phys. Chem.* **1995**, *99*, 14340. Kamitakahara, A.; Pranata, J. *J. Mol. Struct.* **1998**, *429*, 61.
(14) Cho, S. J.; Cui, C.; Lee, J. Y.; Park, J. K.; Suh, S. B.; Park, J.; Kim, B. H.; Kim, K. S. *J. Org. Chem.* **1997**, *62*, 4068.
(15) Bakowies, D.; Kollman, P. A. *J. Am. Chem. Soc.* **1999**, *121*, 5712.
(16) Wu, C.-C.; Jiang, J. C.; Hahndorf, I.; Chaudhuri, C.; Lee, Y. T.; Chang, H.-C. *J. Phys. Chem. A* **2000**, *104*, 9556.
(17) Fogarasi, G.; Szalay, P. G. *J. Phys. Chem. A* **1997**, *101*, 1400.
(18) Perrin, C. L. *Acc. Chem. Res.* **1989**, *22*, 268.
(19) Brown, R. S.; Bennet, A. J.; Slebocka-Tilk, H. *Acc. Chem. Res.* **1992**, *25*, 481.
(20) Lovas, F. J.; Suenram, R. D.; Fraser, G. T.; Gillies, C. W.; Zozom, J. *J. Chem. Phys.* **1988**, *88*, 722.
(21) Meot-Ner, M.; Speller, C. V. *J. Phys. Chem.* **1986**, *90*, 6616.
(22) Wang, Y.-S.; Chang, H.-C.; Jiang, J. C.; Lin, S. H.; Lee, Y. T.; Chang, H.-C. *J. Am. Chem. Soc.* **1998**, *120*, 8777.
(23) Frisch, M. J.; Trucks, G. W.; Schlegel, H. B.; Scuseria, G. E.; Robb, M. A.; Cheeseman, J. R.; Zakrzewski, V. G.; Montgomery, Jr., J. A.; Stratmann, R. E.; Burant, J. C.; Dapprich, S.; Millam, J. M.; Daniels, A. D.; Kudin, K. N.; Strain, M. C.; Farkas, O.; Tomasi, J.; Barone, V.; Cossi, M.; Cammi, R.; Mennucci, B.; Pomelli, C.; Adamo, C.; Clifford, S.; Ochterski, J.; Petersson, G. A.; Ayala, P. Y.; Cui, Q.; Morokuma, K.; Malick, D. K.; Rabuck, A. D.; Raghavachari, K.; Foresman, J. B.; Cioslowski, J.; Ortiz, J. V.; Stefanov, B. B.; Liu, G.; Liashenko, A.; Piskorz, P.; Komaromi, I.; Gomperts, R.; Martin, R. L.; Fox, D. J.; Keith, T.; Al-Laham, M. A.; Peng, C. Y.; Nanayakkara, A.; Gonzalez, C.; Challacombe, M.; Gill, P. M. W.; Johnson, B.; Chen, W.; Wong, M. W.; Andres, J. L.; Gonzalez, C.; Head-Gordon, M.; Replogle, E. S.; Pople, J. A. *Gaussian 98*, Revision A.5; Gaussian, Inc.: Pittsburgh, PA, 1998.
(24) Jiang, J. C.; Chang, H.-C.; Lee, Y. T.; Lin, S. H. *J. Phys. Chem. A* **1999**, *103*, 3123.
(25) Jiang, J. C.; Chang, J.-C.; Wang, B.-C.; Lin, S. H.; Lee, Y. T.; Chang, H.-C. *Chem. Phys. Lett.* **1998**, *289*, 373.
(26) Detailed geometry information concerning the bond angles and lengths of all the isomers considered in text is available on the World Wide Web at http://po.iams.sinica.edu.tw/lab/hcchang/wcche/index.html.
(27) Hunter, E. P. L.; Lias, S. G. *J. Phys. Chem. Ref. Data* **1998**, *27*, 413.
(28) Chang, H.-C.; Jiang, J. C.; Hahndorf, I.; Lin, S. H.; Lee, Y. T.; Chang, H.-C. *J. Am. Chem. Soc.* **1999**, *121*, 4443.
(29) Masella, M.; Flament, J. P. *J. Chem. Phys.* **1998**, *108*, 7141 and references therein.
(30) Gu, Y.; Kar, T.; Scheiner, S. *J. Am. Chem. Soc.* **1999**, *121*, 9411 and references therein.
(31) Wu, C.-C.; Jiang, J. C.; Boo, D. W.; Lin, S. H.; Lee, Y. T.; Chang, H.-C. *J. Chem. Phys.* **2000**, *112*, 176.
(32) Jiang, J. C.; Wang, Y.-S.; Chang, H.-C.; Lin, S. H.; Lee, Y. T.; Chang, H.-C. *J. Am. Chem. Soc.* **2000**, *122*, 1398.
(33) Ciobanu, C. V.; Ojamäe, L.; Shavitt, I.; Singer, S. J. *J. Chem. Phys.* **2001**, *113*, 5321.
(34) Tuckerman, M. E.; Laasonen, K.; Sprik, M.; Parrinello, M. *J. Chem. Phys.* **1995**, *103*, 150. Marx, D.; Tuckerman, M. E.; Hutter, J. G.; Parrinello, M. *Nature* **1999**, *397*, 601.
(35) Mulliken, R. S. *J. Chem. Phys.* **1955**, *23*, 2833.
(36) A full analysis of the potential minima and transition states is beyond the scope of this paper and will be presented elsewhere.
(37) Attempts have also been made to obtain the spectra of O-protonated *N*-methylformamide (NMF)−water clusters. The spectrum of H^+NMF-$(H_2O)_3$ is in general similar to that of $H^+FA(H_2O)_3$ (Figure 3), except that the free-NH stretch of the NMF hydrogen-bonded to an H_3O^+ ion core is resonant at ∼3480 cm^{-1}, in close agreement with that of the neutral *N*-methylformamide isolated in the gas phase (Jones, R. L. *J. Mol. Spectrosc.* **1958**, *2*, 581).
(38) Meot-Ner, M. *J. Am. Chem. Soc.* **1984**, *106*, 278.
(39) Klassen, J. S.; Blades, A. T.; Kebarle, P. *J. Phys. Chem.* **1995**, *99*, 15509.
(40) Rodriguez-Cruz, S. E.; Klassen, J. S.; E. R. Williams, *J. Mass Spectrom.* **1997**, *8*, 565.
(41) Jarrold, M. F. *Acc. Chem. Res.* **1999**, *32*, 360.
(42) Hill, R. L. In *Advances in Protein Chemistry*; Anfinsen, C. B.; Anson, M. L.; Edsall, J. T.; Richards, F. M., Eds.; Academic Press: New York, 1965; p. 37.